A Scalar Function formulation for Optical Flow: Applications to X-ray Imaging

Amir A. Amini
Departments of Diagnostic Radiology and Electrical Engineering
Yale University
New Haven, CT 06510

Abstract

In this work, we present results from a new formulation for determining cross sectional blood velocities from a time-sequence of X-ray projection arteriograms. Starting with the conservation of mass principle, and physics of X-ray projection, we derive a motion constraint equation for projection imaging, a practical special case of which is shown to be the Horn and Schunck's optical flow constraint. We are interested in the study of non-rigid motion of blood which is an incompressible fluid, and as such have developed a formulation for optical flow which is applicable to such media. The formulation is particularly efficient, as the flow field is obtained from a 90 degrees rotation applied to the gradient of a scalar function. It is shown that if specific criteria are met, in addition to normal flow which is commonly recoverable, the tangential component of flow is also recoverable, without the need for smoothness. An algorithm is presented to illustrate this. Preliminary results from the optical flow formulation applied to synthetic images, as well as contrast-injected X-ray images of flowing fluid, in a cylindrical vessel phantom are presented.

1 Introduction

In the past, much of the work in image sequence analysis in the field of computer vision has dealt with analysis of motion of rigidly moving objects [1]. Non-rigidity however occurs abundantly in the motion of solid structures: motion of trees, muscular motion of faces, and non-rigid movement and pumping motion of the left-ventricle (LV) of the heart [11, 9, 3, 4, 12, 13]. In this paper, we discuss new machinery applicable to non-rigid motion analysis of incompressible fluids. In case of fluids, such as the blood, the clear direction is to develop methods capable of estimating the velocity field at all points within the fluid body.

In clinical, and medical imaging literature, methods for quantifying blood flow have received a great deal of attention. This is not surprising as atherosclerotic disease is at the root of heart attacks and strokes, and is still considered the number one killer in the US. Also, its manifestation in other arteries such as the femoral or illiac arteries can lead to loss of limbs and organs. As a result it is quite crucial to diagnose, locate, and accurately quantitate the severity of vessel blockage, and in case of PCTA or PTA (balloon angioplasty) to evaluate the effectiveness of such interventional procedures. There is on-going work in ultrasound [7], X-ray angiography [6], and nuclear magnetic resonance [5] for development of techniques for blood flow quantitation. Methods for computation of velocity field from X-ray imaging, more closely relates to techniques presented in this paper are discussed in [8, 15].

In this paper, we formulate a new framework for optical flow, and apply it to measurement of non-rigid motion of blood from a sequence of X-ray projection images. The paper is organized into two parts. In the first part, a general motion constraint equation for X-ray projection imagery is derived. It is shown that Horn and Schunck's optical flow constraint is a special case of this more general constraint. To derive this equation, the conservation of mass principle is applied to flowing blood and the injected contrast medium in a vessel in order to obtain an equation which related partial derivatives of a sequence of X-ray projection pictures with image velocities. In the second part, the scalar function formulation for optical flow is presented. The novel aspects of this formulation are itemized below:

- The basis for the formulation is computation of a 2D scalar function, allowing for the divergence-free constraint to be exactly enforced.
- As opposed to computing both the x and y components of velocities, we only need to compute a single scalar function, providing for computational savings.
- Methods are applicable to both two and three dimensional images. The extension of the 2D formulation to 3D images assumes axi-symmetric motion.

2 Motion Constraint Equation for X-ray Imaging

We start by applying the conservation of mass principle to flowing blood in a non-branching vessel phantom. We will refer to density of blood as ρ_b, and assume that ρ_b is constant, the requirement for an incompressible fluid [14]. Then, in any given region of interest in a vessel, the rate of change of amount of blood mass must be the same as the amount of flux of blood mass across the boundary of that region, so that we have:

$$\frac{\partial}{\partial t}\int \rho_b dA + \int_{\partial A} (\rho_b \vec{v}.\vec{n}) ds = 0 \qquad (1)$$

where $\vec{v}$ is the blood velocity, n is normal to the boundary of the region ∂A, and ds is the differential of length element along the boundary of region. The second integral along ∂A is the blood mass flux. Upon invoking Gauss's theorem, we have the continuity equation involving blood density and blood velocity:

$$\frac{\partial \rho_b}{\partial t} + \nabla \cdot (\rho_b \vec{v}) = 0 \tag{2}$$

with ρ_b constant, the above equation simplifies to

$$\nabla \cdot \vec{v} = 0 \tag{3}$$

which is the condition for incompressibility of blood, the divergence free constraint. In X-ray imaging, blood will not be visible in itself, and a contrast material must be injected in to the blood stream with a catheter when imaging the vessel, resulting in attenuation of the X-rays. The contrast velocity will obey blood velocity, $\vec{v}$,

$$\frac{\partial \rho_c}{\partial t} + \nabla \cdot (\rho_c \vec{v}) = 0 \tag{4}$$

Since the divergence of blood velocity must be zero, the above equation reduces to

$$\frac{\partial \rho_c}{\partial t} + \vec{v} \cdot \nabla \rho_c = 0 \tag{5}$$

Assuming monochromatic X-ray beams, for X-ray projection imaging,

$$\log \frac{E}{E_0} = -\left\{ BL(l) + \int_0^l \mu_c \rho_c(\beta(u)) |\beta'(u)| du \right\} \tag{6}$$

where $E = E(\beta(l))$ is the image intensity that results when one follows the actual path of an X-ray beam up to the point $\beta(l) = (x(l), y(l), z(l))$, u parametrizes the X-ray beam path through the phantom, E_0 denotes the unattenuated X-rays, μ_c is the mass attenuation coefficient of contrast material and $L(l)$ is the length of path traversed by the beam. B is used to denote the combined attenuation effects in the absence of contrast material. Given this relationship, one can obtain the actual contrast material density at a point, assuming the X-ray beam travel a straight path from a source point, $x_s, y_s, z_s)$:

$$\rho_c(x,y,z) = \frac{1}{\mu_c} \left\{ \frac{-\nabla E}{E} \right\} \cdot \frac{((x-x_s),(y-y_s),(z-z_s))}{\sqrt{(x-x_s)^2 + (y-y_s)^2 + (z-z_s)^2}} - \frac{B}{\mu_c} \tag{7}$$

The above equation may be substituted back into (5) to result in a general equation in terms of E, and the components of the vector in the direction of the X-ray beam emanating from the source at (x_s, y_s, z_s). If the source can be assumed to emanate parallel beams, $\rho_c(x,y,z) = -\frac{1}{\mu_c}\left\{B + \frac{E_t}{E}\right\}$, resulting in the following equation of continuity for the intensity in terms of blood velocities

$$E_z E_t - E E_{zt} + (E_x E_z - E E_{xz})u + (E_y E_z - E E_{yz})v + (E_z^2 - E E_{zz})w = 0 \tag{8}$$

where partial derivatives are taken with respect to x, y, z, t; all subscripted accordingly. In addition, u,v, and w are each functions representing the x, y, and z components of $\vec{v}$ at a point.

With a 2D flow approximation of 3D blood flow, $w = 0$. Furthermore, if we assume that on the average, the distribution of contrast mass can be described by a 2D function, $\rho_c(x,y,z) = \rho_c(x,y)$. The following equation is then obtained as a special case of equation (8):

$$E_t + uE_x + vE_y = 0 \tag{9}$$

describing the components of blood velocities in terms of partial derivatives of contrast-injected pictures. Note that the above equation is the well-known Horn and Schunck's optical flow constraint and related the partial derivatives of a sequence of images at a point, with the velocity of points on a moving object [10]. Here, we have shown a general form of this equation for X-ray images starting from the conservation of mass principle, and derived (9) as a practical special case for our application. In passing, we note that the natural extension of (9) to 3-space may be directly applied to 3D imaging methods.

3 Scalar Function Formulation

The formulation is based on computing a stream function that approximately enforces a constraint of the form given in equation (9) for the blood velocity field, and at the same time the incompressibility condition is readily and exactly satisfied. In 2D, one can always define a scalar function Ψ such that the velocity field is expressed as

$$\vec{v} = \hat{z} \times \nabla \Psi \tag{10}$$

where $\hat{z}$ is a unit vector perpendicular to the image plane. It can easily be checked that this vector field satisfies the divergence free property. We will refer to such a function as a stream function. In 3D, a similar function may be defined for axi-symmetric flow.

Note that in the dual problem one determines a curl-free velocity field. Parallel to the definition of stream function Ψ, which provides divergence-free velocity fields, we can define a velocity potential Φ, with

$$\vec{v} = \nabla \Phi \tag{11}$$

The curl of $\vec{v}$, $\nabla \times \nabla \Phi = 0$. This formulation will be suitable for study of irrotational flow fields.

Substitution of components of (10) into equation (9) results in the following hyperbolic PDE:

$$\Psi_x E_y - \Psi_y E_x + E_t = 0 \tag{12}$$

which is a first order equation whose characteristics [2] are the level curves of the projection pictures, E.

We can perform the following integration along a curve C in order to invert equation (12):

$$\Psi(x,y) = \Psi_0 + \int_{(x_0,y_0)}^{(x,y)} \nabla \Psi \cdot \vec{t} ds \tag{13}$$

where Ψ_0 is the value of Ψ at (x_0, y_0) and $\vec{t}$ is the tangent to C. If C is a level curve of E, the above integral

provides an algorithm for determining the mass flux:

$$\Psi(x,y) = \Psi_0 + \int_{(x_0,y_0)}^{(x,y)} \frac{-E_t}{|\nabla E|} ds \tag{14}$$

Along level curves which wrap around, the integral sum in (14) must vanish. As this is very much data dependent, in general such curves will give rise to singularities in the numerical solution.

3.1 Regularized Solution

Since it is difficult to predict the behavior of the level curves, a more stable numerical algorithm will involve a least-squares solution with an associated variational principle for finding the stream function Ψ:

$$J[\Psi] = \int\int (\Psi_x E_y - \Psi_y E_x + E_t)^2 + \lambda(\Psi_{xx}^2 + 2\Psi_{xy}^2 + \Psi_{yy}^2) dx dy \tag{15}$$

so that J is minimized. The parameter λ controls the degree of smoothing, and in general is a non-negative function of x and y.

Discretizing the above integral on the pixel grid, we obtain a sum with central difference approximations for partial derivatives of Ψ, as well as partial derivatives of $E(x,y)$. Solution of the minimization problem at each pixel is obtained by SOR [2].

As Ψ can only be determined up to an additive constant, we set $\Psi = 0$ on the lower boundary and $\Psi = \Gamma$ on the upper boundary. The latter quantity is the total mass flux in a given vessel with no branchings and may be determined using (14), or with a second variational principle involving Γ.

3.2 Experimental Results

We have performed simulations to validate the promise of the technique in computing velocity fields from X-ray angiograms.

The following 2D simulation involved generating a sequence of images where all the models were identically satisfied. For generating synthetic data, we assumed, $\Psi(x,y) = \frac{y}{Y}\Gamma$, with $y \in [0,Y]$ so that $\vec{v} = (-\frac{\Gamma}{Y}, 0)$. This would be the case for example, for inviscid flow. We also assumed, $E(x,y) = -\frac{E_0}{X} \cdot x(x-X)$, with $x \in [0,X]$ so that $E_t = -\vec{v} \cdot \nabla E = \frac{-2\Gamma E_0}{XY}x + \frac{E_0\Gamma}{Y}$. Using central difference approximation, we then have, $E(x,y,t+\Delta t) = 2\Delta t E_t + E(x,y,t-\Delta t)$. With E_t as given, we generated the first few frames in the sequence with $\Gamma = 128$, $E_0 = 4$, and $X = Y = 128$. Note that in this case at $x = \frac{X}{2}$ the image gradient vanishes. The results from the algorithm are shown in figure 1.

We have just begun with our *in vitro* experiments. The experimental model is a latex tube with an inner diameter of 1.27 cm. X-ray angiography is performed on a GE Advantx digital imaging system at the 6″ image intensifier field, with 1024 × 1024 acquisitions at rapid frame rates. For the experiment shown in figure 2, a pump delivered 612 ml/min of water in the continuous flow mode, and 5 ml/sec of an iodine contrast agent was injected for 2 seconds. In order to assess the overall effectiveness of the methodology, soon we will be carrying out statistical testing of the velocity field measurements against known velocities and volumetric flow rates. Further *in vitro* validations of methods and integration with MR-based flow estimation techniques are also planned.

4 Conclusions

In this paper, we have presented results from a new formulation for optical flow. The formulation is computationally efficient, as one needs to only compute a single scalar function, with the prerequisite that either the global curl or divergence of the flow field is identical to zero. We discussed sources for numerical instabilities, and linked such behavior with wrap around of level curves of E. In fact, along well-behaved level curves, in principle, one can integrate the Horn and Schunck optical flow constraint. Note that this statement has deeper implications: that is, in addition to the normal component of the velocity field, in the absence of bad characteristics, the tangential component of the velocity field is recoverable, bypassing the aperture problem.

References

[1] J. K. Aggarwal. Motion and time-varying imagery – an overview. In *Proceedings of the Workshop on Visual Motion*, 1986.

[2] William F. Ames. *Numerical Methods for Partial Differential Equations.* Academic Press, New York, 1992.

[3] A. A. Amini, R. W. Curwen, R. T. Constable, and J. C. Gore. Mr physics-based snake tracking and dense deformations from tagged cardiac images. In *AAAI Symposium on Applications of Computer Vision to Medical Image Processing*, Stanford University, Stanford, California, March 21-23 1994.

[4] A. A. Amini and J. S. Duncan. Bending and stretching models for lv wall motion analysis from curves and surfaces. *Image and Vision Computing*, 10(6):418–430, July/August 1992.

[5] William G. Bradley. Flow phenomena in mr imaging. *American Journal of Radiology*, 150:983–994, 1988.

[6] A. M. Seifalian et al. Validation of a quantitative radiographic technique to estimate pulsatile blood flow waveforms using digital subtraction angiographic data. *J. Biomedical Engineering*, 13:225–233, 1991.

[7] R. I. Kitney et al. 3d visualization for the study of arterial disease and tissue characterization. In *Proc. of Computers in Cardiology*, 1991.

[8] J. M. Fitzpatrick. A method for calculating velocity in time dependent images based on the continuity equation. In *Proceedings of IEEE Conference on Computer Vision and Pattern Recognition*, pages 78–81, San Francisco, 1985.

[9] D. Goldgof, H. Lee, and T. Huang. Motion analysis of nonrigid surfaces. In *Proceedings of IEEE conference on Computer Vision and Pattern Recognition*, 1988.

[10] B.K.P. Horn and B. G. Schunck. Determining optical flow. *Artifical Intelligence*, 1981.

[11] T. Huang. Modeling, analysis, and visualization of nonrigid object motion. In *International Conference on Pattern Recognition*, 1990.

[12] D. Metaxas and D. Terzopoulos. Recursive estimation of shape and nonrigid motion. In *IEEE Workshop on Visual Motion*, pages 306–311, 1991.

[13] C. Nastar and N. Ayache. Non-rigid motion analysis in medical images: A physically based approach. In *Information Processing in Medical Imaging*, pages 17–32, 1993.

[14] R. Peyret and T. D. Taylor. *Computational Methods for Fluid Flow.* Springer-Verlag, New York, 1985.

[15] S. M. Song and R. M. Leahy. Computation of 3d velocity fields from 3d cine-ct images of a human heart. *IEEE Transactions on Medical Imaging*, 10(3):295–306, 1991.

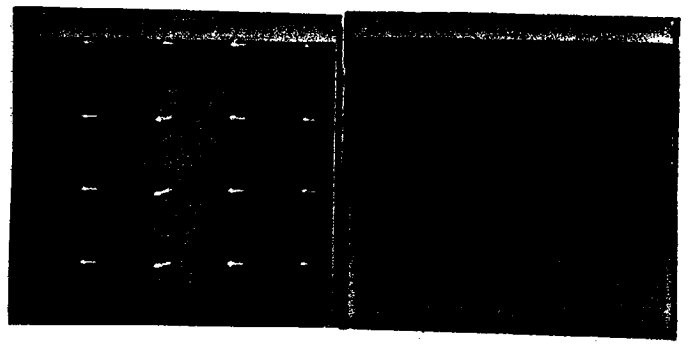

Figure 1: Sampled velocity field overlaid on the second picture of a simulated sequence for left translating flow. The computed stream function is shown on the right.

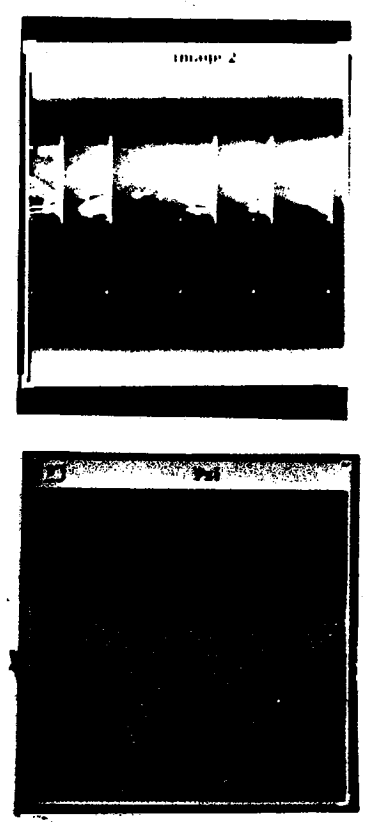

Figure 2: Top: cross-sectional velocity profiles computed from 3 frames in a phantom sequence, overlaid on the middle frame. Note that the picture is displayed in *reverse video*. Bottom: The computed stream function from 3 frames is shown next.